Expanded View Figures

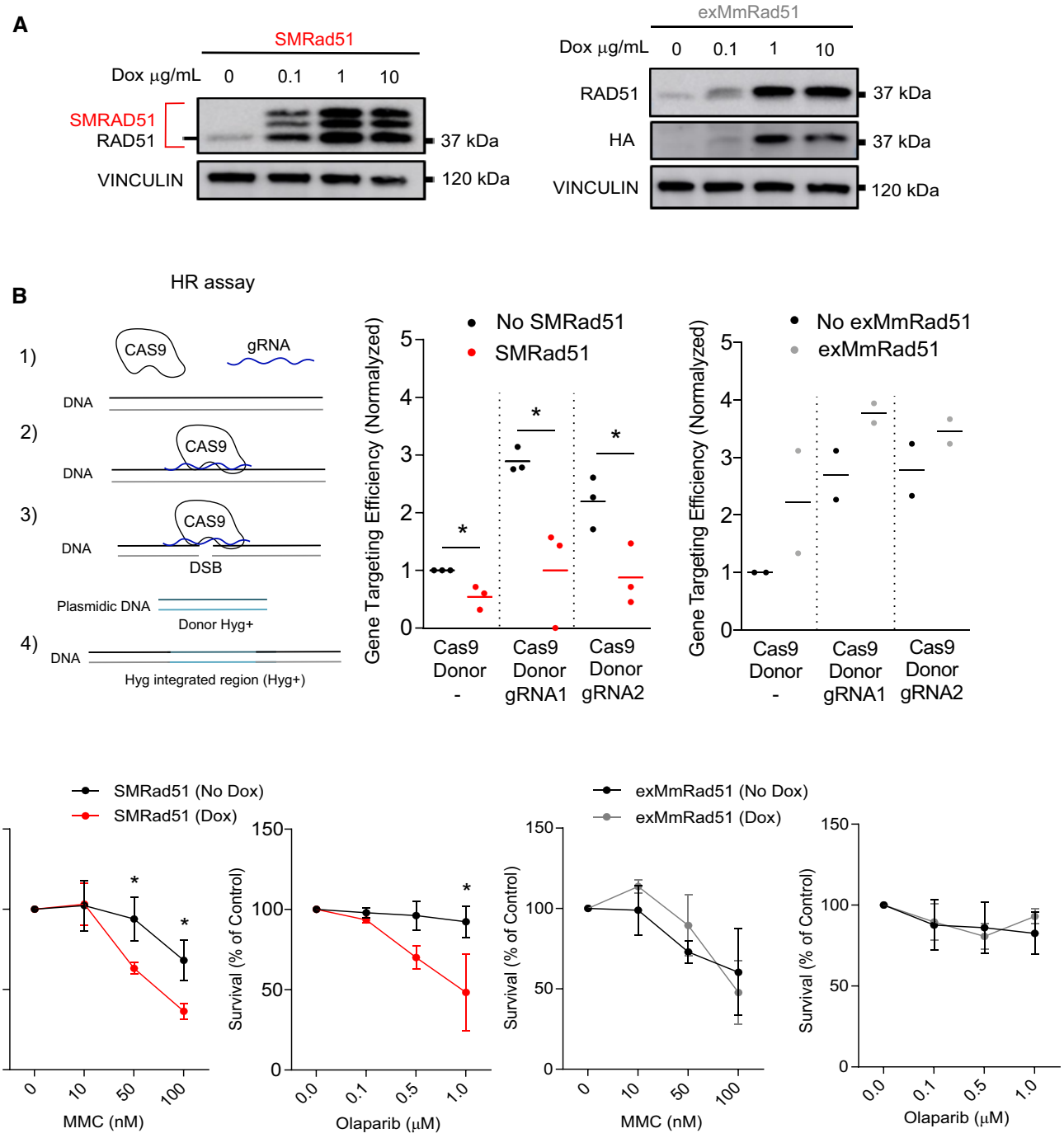

Figure EV1.

Figure EV1. *SMRad51* expression decreases HR efficiency and increases sensitivity to genotoxic agents in immortalized MEFs.

A Transgene expression as assessed by Western blot analysis in immortalized exMmRad51 or SMRad51 MEFs treated or not treated with increasing concentrations of Dox for 24 h. SMRAD51 expression resulted in 3 characteristic diagnostic bands (Lambert & Lopez, 2000, 2001; Saintigny *et al*, 2001; Wilhelm *et al*, 2014; So *et al*, 2022).

B Homology-directed repair-mediated gene targeting assay. The protocol consisted of sequence homology-dependent replacement of the second exon of the 53BP1 gene by a hygromycin resistance (Hyg^{+}) gene using homologous donor DNA (here called Donor) after Cas9-mediated induction of a DSB in the targeted sequence (left panel). Cells with and without SMRad51 expression were transfected with three combinations of plasmids: (1) Cas9+Donor (no Cas9 activity) and (2) Cas9+Donor+gRNA1 (Cas9 active) or (3) Cas9+Donor+gRNA2 (Cas9 active). Recombinant cells became resistant to hygromycin. Right panel: Quantification from 3 independent experiments.

C Quantification of cell viability by colony formation assay for immortalized MEFs expressing or not expressing SMRad51 or exMmRad51 observed 10 days after MMC or Parp inhibitor (olaparib) treatment. Dox treatment was started 24 h before exposure to genotoxic drugs. Statistical analysis: (B) Student's *t*-test. (C) Two-way ANOVA followed by Sidak posttest, Student's *t*-test. $*P < 0.05$. The error bars represent the ±SEM.

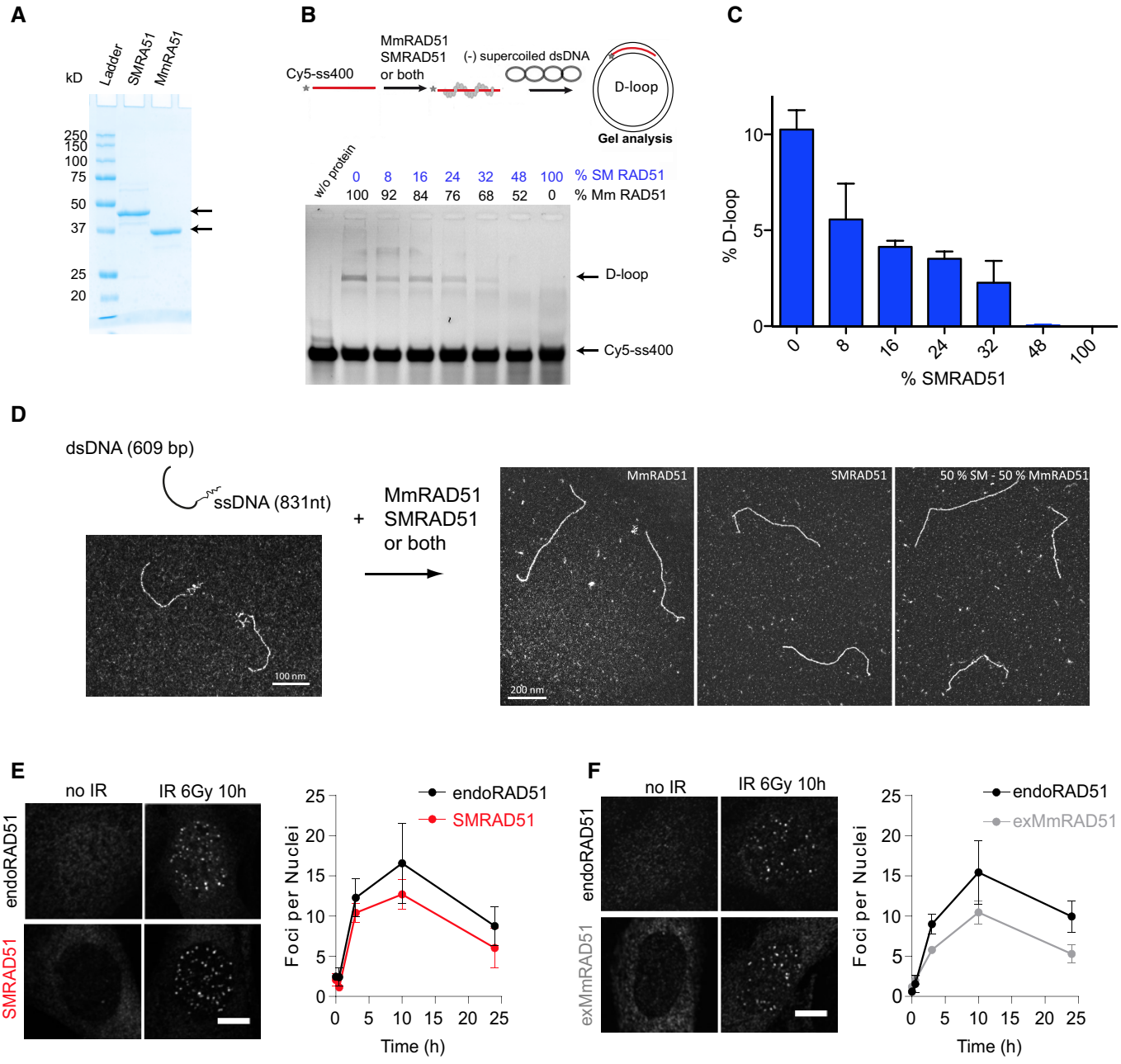

Figure EV2.

Figure EV2. Cellular and biochemical characterization of SMRAD51.

A Electrophoresis analysis of the purified SmRAD51 and MmRAD51 proteins.

B Impact of SMRAD51 on the MmRAD51-mediated D-loop assay. Upper panel: scheme of the D-loop assay. Lower panel: gel electrophoresis of the D-loop formation experiment. Lane 1: in the absence of proteins; other lanes: different mix of MmRAD51 and SMRAD51 proteins. The respective percentages of each protein are indicated.

C Quantification of the D-loop assay.

D Transmission electron microscopy (TEM) analysis. Left panel: the DNA substrate. Right panels: representative pictures of presynaptic filaments formed by MmRAD51, SMRAD51 or both. Note that 100% of DNA molecules were coated by MmRAD51 or SMRAD51.

E, F Representative pictures and quantification of endogenous MmRAD51 (endoRad51), SMRAD51 and exMmRAD51 focus formation dynamics after irradiation. Immortalized MEFs were treated or not treated with Dox for 24 h, exposed to ionizing irradiation (6 Gy) and fixed at different time points. SMRAD51 was stained with a specific antibody raised against the N-terminal part of yeast ScRad51. exMmRAD51 was stained with an HA-tag antibody. The graph shows the ±SEMs of three independent experiments. EndoRAD51 staining was performed in cells not treated with Dox and stained for RAD51. Scale bars: 5 μm.

Figure EV3. Impact of *SMRad51* expression on alternative nonconservative DSB repair mechanisms SSA and EJ, immortalized MEFs.

A Efficiency of RAD51 silencing (left panel) or *SMRad51* expression (right panel).

B Impact on SSA. Upper panel: reporter substrate monitoring SSA induced by targeted cleavage by the meganuclease I-SceI (Gunn & Stark, 2012). The values are shown normalized to the control siRNA (CT) plus I-SceI and represent the average ± SEM of at least 3 independent experiments.

C Impact on EJ. Upper panel: reporter substrate monitoring EJ induced by targeted cleavage by the meganuclease I-SceI (Guirouilh-Barbat *et al*, 2004, 2007; Rass *et al*, 2009; Gelot *et al*, 2016; So *et al*, 2022). The values are shown normalized to the control siRNA (CT) plus I-SceI and represent the average ± SEM of at least 3 independent experiments. Student *t*-test: $*P < 0.05$ and $**P < 0.01$.

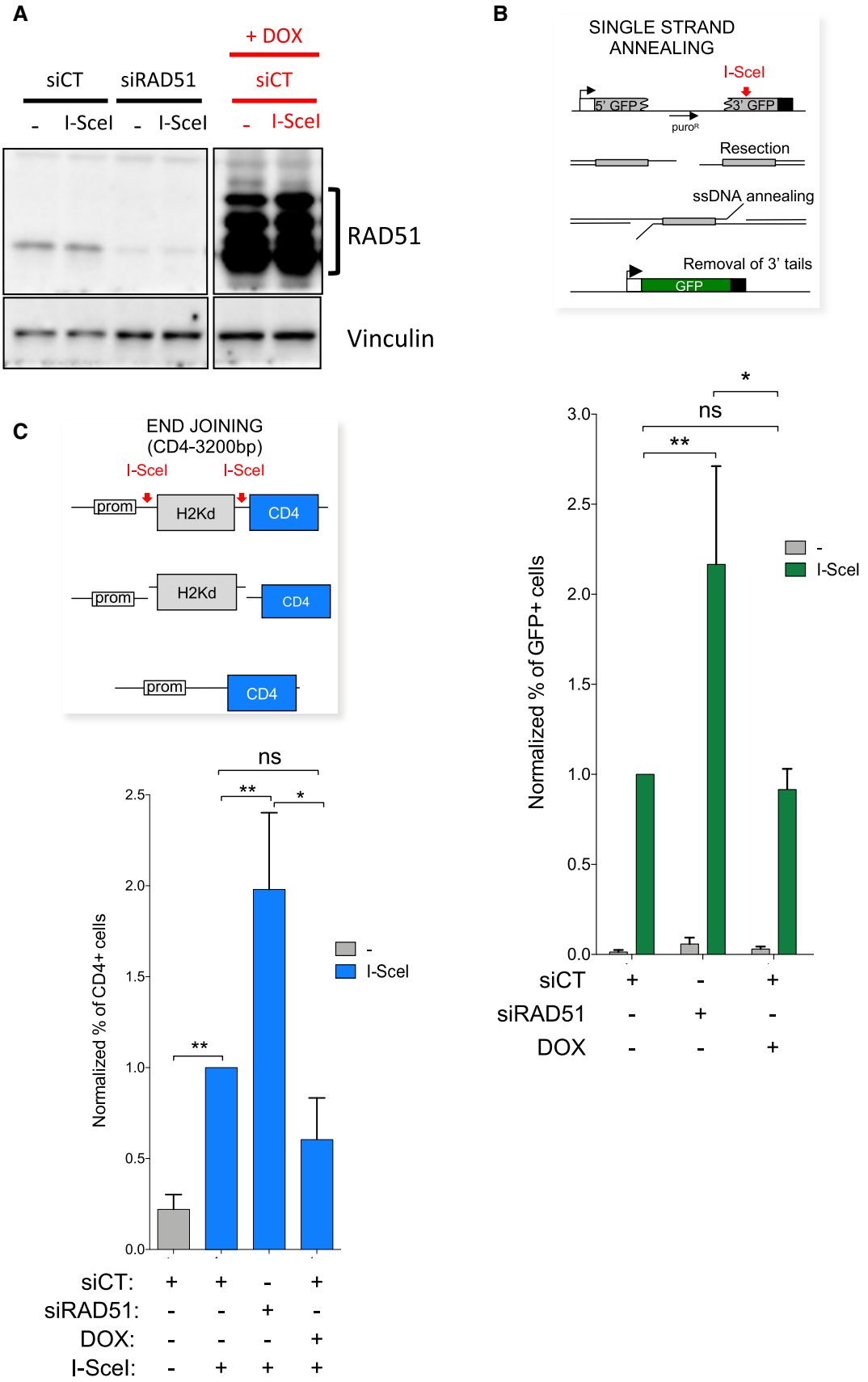
A
+ DOX
siCT
siRAD51
siCT
- I-SceI - I-SceI - I-SceI
RAD51
Vinculin
B
SINGLE STRAND ANNEALING
I-SceI
5' GFP
3' GFP
puroR
Resection
ssDNA annealing
Removal of 3' tails
GFP
C
END JOINING (CD4-3200bp)
I-SceI I-SceI
prom
H2Kd
CD4
Normalized % of CD4+ cells
Normalized % of GFP+ cells
ns
**
*
- I-SceI
siCT: + + - +
siRAD51: - - + -
DOX: - - - +
I-SceI: - + + +
siCT + - +
siRAD51 - + -
DOX - - +

Figure EV3.

A

Organ	Phenotype (SMRad51)
Kidney	Normal histology
Stomach	Normal histology
Pancreas	Normal histology
Heart	Normal histology
Liver	Normal histology
Large Intestine	Normal histology
Small Intestine	Normal histology
Ovary	Normal histology
Spleen	Presence of hematopoietic figures
Testis	Reduced size with normal histology
Lung	Edematous alveolitis
Skin	Squamous epithelium with hyperplasia, atypia and hyperkeratosis (ortho). 1 of 6 mice presented squamous cell carcinoma

B

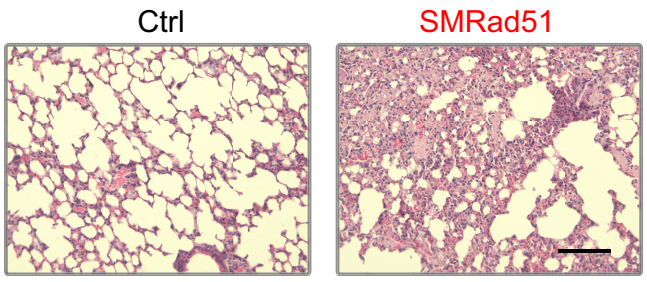

Figure EV4. Histopathological analysis of adult mice after *SMRad51* expression for 3 months.

A Table showing a summary of the pathological analysis results for various tissues of Ctrl and SMRad51 adult mice fed a Dox-containing diet for 6 months. At least 3 different mice of each genotype were analyzed.

B Representative images of hematoxylin–eosin-saffron staining in lungs. Scale bar: 100 μm.

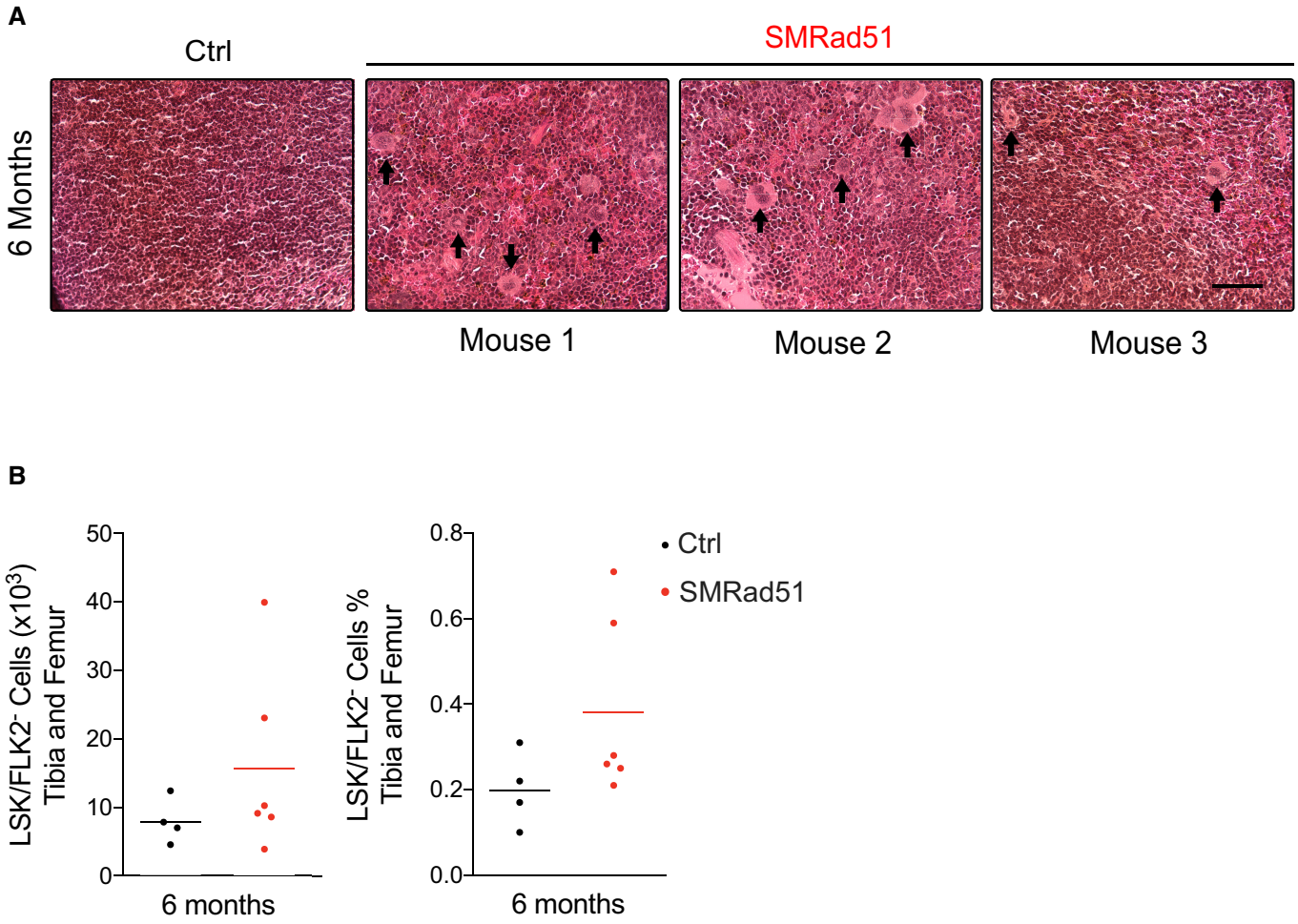

Figure EV5. Expression of *SMRad51* in adult mice leads to extramedullary hematopoiesis in the spleen, increases hematopoietic stem cells in the bone marrow and leads to DNA damage in the small intestine.

A Representative images of hematoxylin–eosin-saffron staining in spleen sections of Ctrl and SMRad51 adult mice fed a Dox-containing diet for 6 months. Arrows: overrepresentation of megakaryocytes in the spleens of *SMRad51*-expressing mice.

B Quantification of hematopoietic stem cells Lin (–), Sca-1 (+), c-Kit (+) and FLK2 (–) (in short, LSK/FLK2–) in tibia and femur of Ctrl (n = 4) and SMRad51 (n = 6) adult mice fed with Dox-containing diet for 6 months. In the left, the absolute number of cells was plotted. In the right, the percentage of cells was plotted. Each point in the graphs represents an independent biological replicate and the horizontal bar show the mean. (A) Scale bar: 100 μm.